Indian Journal of Chemistry
Vol. 63, May 2024, pp. 506-517
DOI: 10.56042/ijc.v63i5.9396

Molecular docking and dynamic simulation analysis of natural polyphenols for identifying potential PTP1B inhibitors for type 2 diabetes

Pratik Khona & Uma Kabra*

Department of Pharmaceutical Chemistry, Parul Institute of Pharmacy, Parul University, Vadodara, Gujarat, India

E-mail: uma.kabra16205@paruluniversity.ac.in

Received 8 March 2024; accepted(revised) 25 April 2024

Type 2 diabetes (T2D) is a complex illness and a significant source of morbidity and mortality globally. Insulin resistance is characterized by defect in insulin signaling pathway. Development of novel therapeutic agent that can improve insulin resistance could be beneficial for the treatment of T2D. Activation of insulin receptor involves phosphorylation of its tyrosine residues. However, dephosphorylation of these residues by protein tyrosine phosphatases reduces the insulin receptor kinase activity. PTP1B negatively regulate insulin signaling and leptin signaling pathways. Naturally occurring polyphenols can improve insulin resistance by a range of actions, including lowering postprandial blood sugar levels, modulating the signaling of insulin pathways, and sparing insulin-secreting pancreatic β-cells from harm. Therefore, in the present study we screened natural polyphenol from phenol explorer library using molecular docking and molecular dynamics simulation techniques to predict possible PTP1B inhibitors. Our virtual molecular docking data have showed that ten natural polyphenol compounds displayed stronger binding affinity and essential amino acid interaction toward the PTP1B inhibitory site. Further, molecular dynamics simulation findings have indicated that Theaflavin 3,3'-O-digallate (136), Naringin 4'-O-glucoside (216), and Naringin 6'-malonate (217), exhibit a significant number of dynamic features such as stability, flexibility and binding energy. Our *in silico* analysis shows that the above listed natural polyphenols may potentially be used as PTP1B inhibitor for the management of T2D.

Keywords: Protein tyrosine phosphatase 1B, Polyphenols, Type 2 diabetes, Insulin resistance, Molecular docking, Molecular dynamic simulation

Diabetes Mellitus (DM) is a widespread metabolic disorder characterized by sustained high blood sugar levels and is associated with several co-morbidities like cardiovascular diseases, cancer, obesity, sleep disorder and dyslipidemia[1]. According to International Diabetes Federation, DM has become a global health challenge with a prevalence of 536 million diabetic patient worldwide. Furthermore, the cases are exponentially increasing and projected to rise 783 million by 2045[2]. Insulin resistance (IR) and pancreatic beta cell dysfunction are the pivotal factors contributing to the development and progression of Type 2 DM (T2DM)[3,4]. In IR, peripheral tissues like skeletal muscle, adipose tissue and liver fails to respond adequately to physiological insulin levels, meaning reduced insulin sensitivity due to dysregulation of insulin signaling pathways. The pathway involves binding of endocrine peptide hormone insulin to the insulin receptors inducing autophosphorylation of the receptor. This triggers recruitment and phosphorylation of insulin receptor substrate followed by activation of downstream IRS1/2-PI3K-AkT pathway[5,6]. This in turn mediate the translocation of GLUT 4 to the plasma membrane and enhances the glucose absorption and utilization. Various protein tyrosine kinases (PTK) and protein tyrosine phosphatases (PTP) are involved in the modulation of the insulin-signaling pathway[7,8]. PTPs are the negative regulators of insulin signaling;they dephosphorylate the tyrosine residues of insulin receptor resulting in IR both *in vitro* and *in vivo*[9]. Several reports demonstrated increased PTP1B expression in insulin sensitive tissues of rodents and humans with T2DM. Further, the evidence that signifies the physiological importance of PTP1B is the fact that complete body and tissue specific PTP1B knockout mice exhibited increased glucose tolerance, insulin sensitivity, insulin secretion as well as resistance to weight gain[10,11]. Cumulatively, PTP1B inhibitors has emerged as a possible therapeutic option for the management of T2DM and its associated complications[12]. Recent research emphasize on discovering potent natural polyphenolsas PTP1B inhibitors. However, due to

structural diversity and tissue definite function of PTP1B, development of selective PTP1B inhibitor is very challenging. Until now, only few PTP1B inhibitors namely Ertiprotafib, JTT-551 and Trodusquemine has reached the clinical trials but unfortunately discontinued due to poor pharmacokinetic property and high toxicity profile[13]. Hence, there is an urgent need to identify and develop potent and highly selective PTP1B inhibitors to treat T2DM.

Natural products comprise of compounds with various scaffolds and distinctive biological activities that serve as a source for the identification and development of lead compound. Many natural compounds belonging to the class of alkaloids, flavonoids, terpenoids and steroids possessed PTP1B inhibitory activity[14]. Recently it was found that a compound Viscosol (5,7-dihydroxy-3,6-dimethoxy-2-(4-methoxy-3-(3-methyl-2-enyl)phenyl)-4H-chromen-4-one) extracted from the plant *Dodonaea viscosa* inhibited PTP1B activity *in vitro* and *in vivo* [15]. Similarly other compounds like ursolic acid, 1,2,3,6-Tetragaloylglucose, stilbene derivatives isolated from plant Rheum undulatum L, and flavonoids isolated from the roots of the plant *Broussonetia papyrifera* and *G uralensis* also possessed PTP1B inhibitory activity[16–18]. Accumulating evidences highlights the uniqueness of natural products as lead in developing potent PTP1B inhibitors.

Application of computational techniqueslike molecular docking and dynamic simulation in drug discovery and development process has gained insight as it reduces the cost and time of research. Molecular docking techniques is employed to study the atomic interactions between a ligand and a protein and this enable us to characterize the behaviour of ligand in the binding site of target protein and understand different biochemical processes[19]. Molecular docking provides comprehensive information on ligand conformation and binding affinity within the binding sites[20]. On the other hand, molecular dynamics (MD) simulations apply the principle of physics and helps to anticipate how each atom in a molecule migrate over time[21]. These simulations can record various essential biomolecular process, like conformational shift, ligand binding, protein folding, and positions of all of the atoms with accuracy. Notably, such simulations also predict how macromolecules behave at an atomic level to changes such as a mutation, posttranslational modifications, protonation, and addition or deletion of a ligand[22].

In the present study, we screened library of natural polyphenols obtained from Phenol-Explorer database to identify potent and selective PTPB1 inhibitors. 489 natural polyphenols were docked with the target enzyme PTP1B to assess the specific interactions and the binding mode between them. Thereafter, 3 natural polyphenols with the high docking score were subjected to MD simulation to analyse the conformational stability of the docked complex at different time intervals. The schematic workflow of our study is depicted in Fig. 1. Finally, the main finding of our work is discovery of 3 natural polyphenols 136, 216 and 217 as PTP1B inhibitors that could be considered as drug candidate for treating T2DM.

Methodology

Collection and preparation of ligands

489 natural polyphenols were retrieved from Phenol-Explorer database (http://phenol-explorer.eu/)

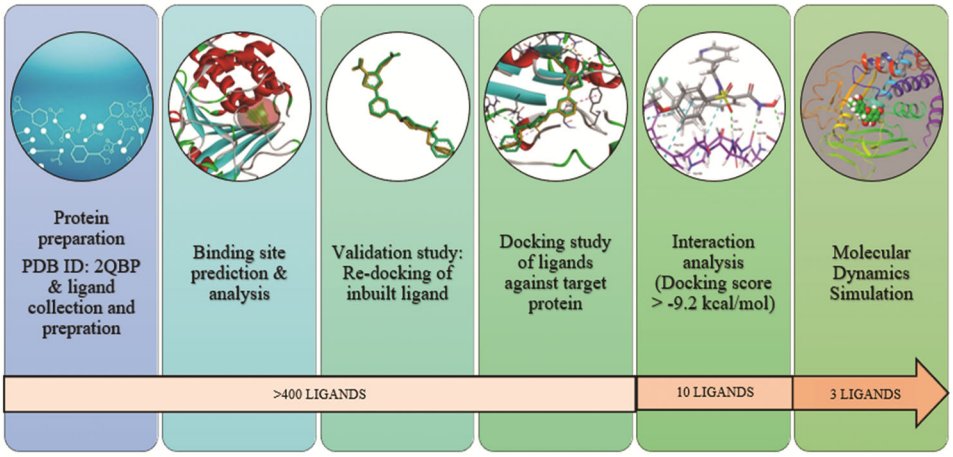

Fig. 1 — The various phases of the screening process of natural polyphenols against PTP1B protein.

in smiles format[23]. All the ligands were converted to protein data bank (PDB) format followed by energy minimization using Open Babel GUI programme and then converted to PDBQT format.

Preparation of protein

The crystal structure of PTP1B having PDB ID: 2QBP, resolution: 2.50 Å was extracted from the RCSB Protein Data Bank (https://www.rcsb.org/) in .pdb format[24]. The protein was pre-processed by removing co-bound ligand, water molecules and adding polar hydrogens and Kollman charges using AutoDock Tools 1.5.7. After pre-processing, the structure obtained was saved in pdbqt format. Visualization of PTP1B crystal structure in BIOVIA Discovery Studio revealed six cavity sites of the protein wherein the cocrystallized (reference) ligand was bound to the site 3[25]. Therefore, site 3 of the protein was considered as the site of inhibition with coordinates as X = 48.164, Y = 10.080 and Z= 3.111.

Docking validation

The validation of the docking procedure was performed by removing the reference ligand inhibitor 527 from the crystal structure of PTP1B and then redocked it into the active site[26]. The amino acid residues namely, ALA217, VAL49, MET258, ALA27, TYR46, LYS120, GLN266, CYS215, SER216, PHE182, GLY259, ARG221 and GLN262 were found in common between re-docked ligand & co-crystallized ligand in BIOVIA Discovery Studio visualizer. Further, the root mean square deviation (RMSD) between re-docked ligand and co-crystallized ligand was calculated.

Multiple ligand docking study

Multiple natural polyphenols were docked against PTP1B protein using AutoDockVina softwareand PADRE & PERL IDE software using vina.pl script[27,28]. The grid size of 41 × 41 × 41 points with a grid spacing of 0.375 Å and exhaustiveness equal to 8 was set for docking. The important active site residues involved in the interaction were explored and binding energy of each protein-ligand complex was determined. The docking models obtained were visualized using BIOVIA Discovery studio software[29].

Molecular dynamic (MD) simulation

After molecular docking, the top three docked complexes with highest binding energy were subjected to MD simulation using Desmond V 2023.2 package with Ubuntu 22.04.3 LTS OS. System builder wizard in the 'Desmond' module was employed to establish the desired system. An orthorhombic simulation box was generated having 10 Å distance between the corners of the box and protein target. Predefined TIP3P solvent model was used to create orthorhombic boundary conditions. Neutralization of the system was carried out by randomly adding counter ions Na^+ and Cl^-. The reduction of solvated protein system was accomplished inside the Desmond protocol by applying OPLS-2005 force field parameters followed by relaxation[30,31].Further, energy minimization of the complex was done by employing the steepest descent method. The Brownian Dynamics NVT ensemble was applied to simulate the system for 100 ps at temperature of 10K for restraining heavy atoms on solute. Molecular dynamics was carried out at temperature 300 K and 1.01 bar pressure using NPT ensemble[32]. To preserve the temperature and pressure scale during dynamic simulation the Nose–Hoover thermostat and the Martyne–Tobias–Klein barostat techniques were employed[33]. The MD simulation was executed for 100 ns, in which 20 ps frame was captured and saved into trajectory. After completion of MD simulation, calculation of root mean square deviation (RMSD), root mean square fluctuation (RMSF), radius of gyration (Rg), number of hydrogen bond and analysis of the interactions shown by complex during entire simulation duration was done[34].

Results and Discussion

In the present study, 489 natural polyphenols compounds were obtained from Phenol-Explorer database and screened through docking against PTP1B protein. Among them, the top 10 ligands with highest negative binding energy were selected for molecular interaction studies with the PTP1B protein. Out of them, the top 3 ligands were subjected to MD simulation studies.

Firstly, the grid generated was validated by redocking the native co-crystal ligand followed by superposition and evaluation of RMSD. The redocking was carried out as shown in Fig. 2. The RMSD value between the reference ligand and redocked ligand was found to be 1.67 Å, indicating that the size and position of the grid generated specifically matches the inhibitor-binding site. Henceforth, docking of all the natural polyphenols

was carried out in the similar way as the validation protocol with same grid box and the data has been supplemented as Table S1. The free binding energy of the natural polyphenols ranged from –5.1 to –9.6 kcal/mol. The free binding energy of the reference ligand inhibitor 527 of PDB ID: 2QBP was –9.6 kcal/mol. The top 10 ligands with highest negative binding energy docked with the PTP1B receptor is shown in Table 1 and were chosen for further study.

Protein Tyrosine Phosphatase 1B enzyme plays a crucial role in cellular signaling by dephosphorylating phosphotyrosine residues on proteins. In T2D, PTP1B enzyme is over expressed, resulting in increased dephosphorylation of insulin receptors and hence insulin resistance in various cells and tissues. Several PTP1B inhibitors entered the clinical trial but failed due to serious side effects and poor selectivity. However, compounds extracted from natural products like terpenoids, alkaloids and flavonoids have been reported to possess potent PTP1B inhibition activity with fewer side effects[35]. The crystal structure of PTP1B consist of 321 residues with 2.5 Å resolution.

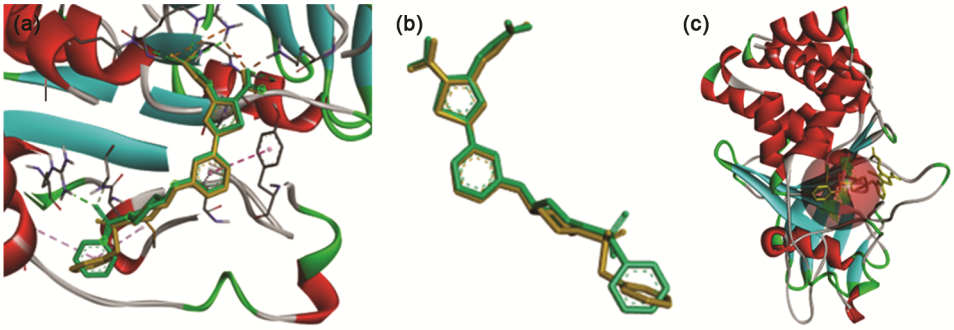

Fig. 2 — Superposition of redocked and the co-crystalized ligand in the protein 2QBP. A) molecular interactions of reference ligand inhibitor 527 with PTP1B receptor. B) superimposition of the reference ligand inhibitors of poses before (yellow) and after docking (green). and C) reference ligand inhibitor 527 docked at the inhibition site (red colour sphere) of PTP1B receptor protein.

Table 1 — Structure and binding energy of top 10 ligands

Compound	Compound ID	Structure	Molecular formula	Binding energy (kcal/mol)
Reference inhibitor 527	IN	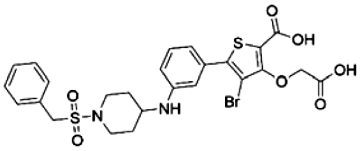	$C_{25}H_{25}BrN_2O_7S_2$	–9.6
Theaflavin 3,3'-O-digallate	136	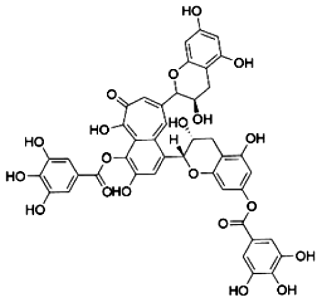	$C_{43}H_{32}O_{20}$	–9.6
Naringin 4'-O-glucoside	216	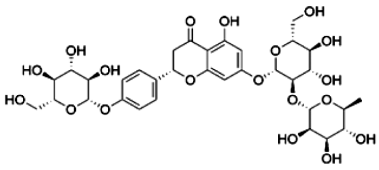	$C_{33}H_{42}O_{19}$	–9.4

(*contd.*)

Table 1 — Structure and binding energy of top 10 ligands (*contd.*)

Compound	Compound ID	Structure	Molecular formula	Binding energy (kcal/mol)
Isorhoifolin	233	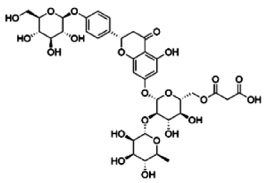	$C_{27}H_{30}O_{14}$	–9.4
24-Methyllathosterol ferulate	565	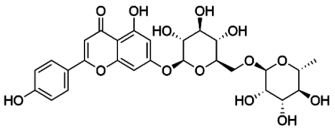	$C_{38}H_{56}O_4$	–9.3
Hesperetin	203	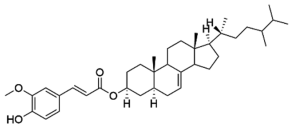	$C_{16}H_{14}O_6$	–9.2
Pinocembrin	220	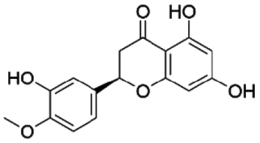	$C_{15}H_{12}O_4$	–9.2
Sesamolin	606	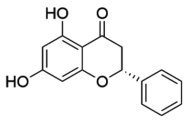	$C_{20}H_{18}O_7$	–9.2
Luteolin 7-O-diglucuronide	239	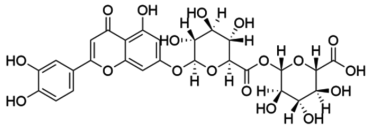	$C_{27}H_{26}O_{18}$	–9.2
Chrysin	240	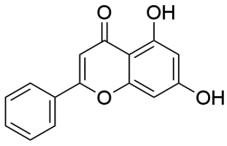	$C_{15}H_{10}O_4$	–9.2
JTT-551	JTT	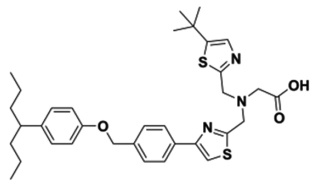	$C_{39}H_{43}N_3O_3S_2$	–7.4

The structural data revealed that PTP1B consist of 5 active sites designated as site A, B, C, D and E. Among them, only site A, B and C are functionally important and thought to regulate insulin signaling[13,36]. The site A is a catalytic domain of PTP1B *i.e.* a phosphate-binding pocket where insulin

receptor kinase gets dephosphorylated[37]. Due to presence of polar residues like CYS215, ARG221, ASP48, GLN262 & 266 and SER 216, the compound that binds only to this pocket exhibit greater potency along with poor selectivity and membrane permeability[38,39]. Although site B is a non-catalytic, binding of compound to this pocket enhances activity and selectivity. The key residues that make up this pocket are ARG254 & 24, MET258, VAL49, GLY259, PHE52, and IIE219. The site C lying adjacent to site A is also a phosphate-binding pocket and amino acid residues like LYS41, TYR46, ARG47 and ASP48 surrounds the pocket. Cumulatively, binding sites B and C surrounds the site A and all the 3 sites play critical role in cell membrane permeability, selectivity and biological activity[40].The molecular interaction exhibited by the reference inhibitor 527 was π–π stacking interaction with residues ALA217, VAL49, MET258, ALA27, TYR46, and H-bond interaction with residues PHE182, GLN266, CYS215, ARG254, SER216, GLY259. Thus, reference inhibitor binds to multiple sites A, B and C. The binding energy and molecular interacting residues with 2D representation of selected 10 natural polyphenols with the PTP1B enzyme (PDB: 2QBP) are shown in Table 2. The binding energy and molecular interactions displayed by polyphenols 136, 216 and 217 were comparable to the reference ligand inhibitor. The docking score of polyphenols 136, 216 and 217 are –9.6 kcal/mol, –9.4 kcal/mol, and –9.4 kcal/mol respectively. All the 3 polyphenols 136, 216 and 217 were found to interact at multiple sites A, B and C that contribute to the selectivity and potency for PTP1B protein. 3D interaction map of PTP1B with IN, 136, 216 and 217 are shown in Fig. 3.

Table 2 — Binding energy and molecular interacting residues with 2D representation of top 10 natural polyphenols with the PTP1B enzyme (PDB: 2QBP).

Compound ID	Binding energy (kcal/mol)	π-π interactions	Hydrogen bond interactions	2D interactions
IN	–9.6	ALA217, VAL49, MET258, ALA27, TYR46, LYS120, ARG221, GLN262	PHE182, SER216, ARG254, CYS215, GLY259, GLN266	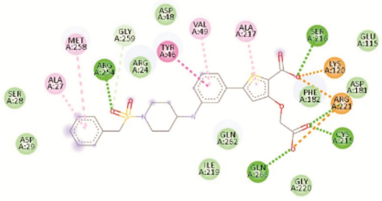
136	–9.6	ARG24, GLY259, ARG254, GLN262, PHE182, SER216, ALA217, ALA27, ASP48	PHE182, SER216, ARG254, GLY259, ARG24, GLN262	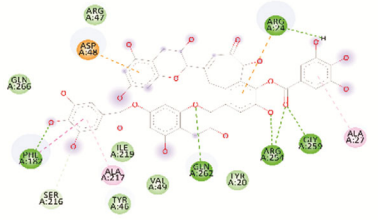
216	–9.4	ALA217, VAL49, TYR46, MET258, LYS120, ASP48	PHE182, SER216, CYS 215, ARG24, ARG221	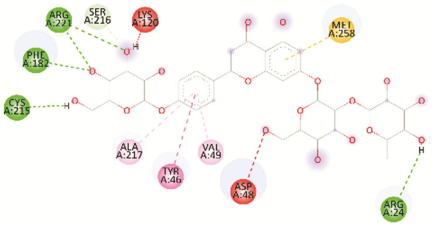

(*contd.*)

Table 2 — Binding energy and molecular interacting residues with 2D representation of top 10 natural polyphenols with the PTP1B enzyme (PDB: 2QBP). (*contd.*)

Compound ID	Binding energy (kcal/mol)	π-π interactions	Hydrogen bond interactions	2D interactions
217	–9.4	ALA217, VAL49, PHE182	PHE182, ARG254, GLN266, ARG24, ARG47, ASP48, LYS36, ASP29, TYR20, LYS120	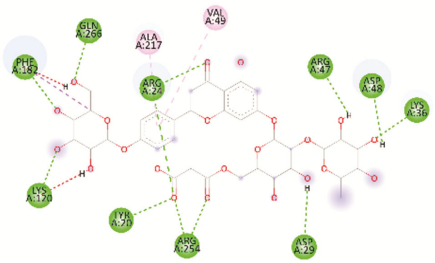
233	–9.4	ALA217, PHE182, VAL49	ARG54, ARG24, ARG221	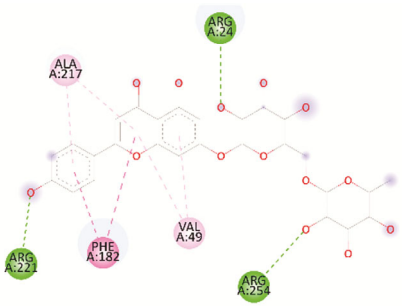
565	–9.3	ALA217, TYR46, LYS41, ARG47, PHE182		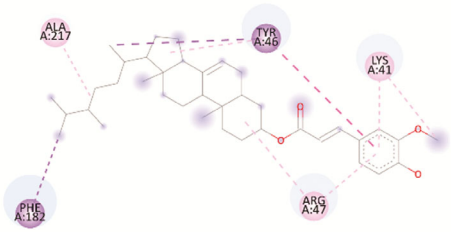
203	–9.2	TYR46, VAL49, ALA217, PHE182	GLN262, GLU115, LYS120, ARG221, ASP48,	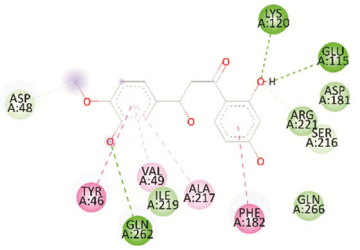
220	–9.2	PHE182, ALA217, VAL49, TYR46	TYR46, LYS120, SER216, ARG221,	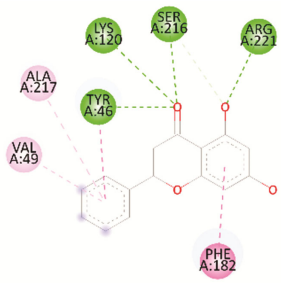

(*contd.*)

Table 2 — Binding energy and molecular interacting residues with 2D representation of top 10 natural polyphenols with the PTP1B enzyme (PDB: 2QBP). (*contd.*)

Compound ID	Binding energy (kcal/mol)	π-π interactions	Hydrogen bond interactions	2D interactions
606	–9.2	PHE182, ALA217	ARG221, ARG24, GLN262	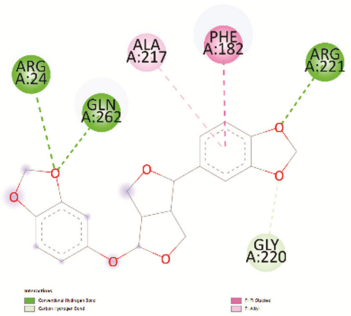
239	–9.2	ALA217, PHE182, VAL49, ASP29	ARG24, GLN262, PHE182, ARG254, SER28	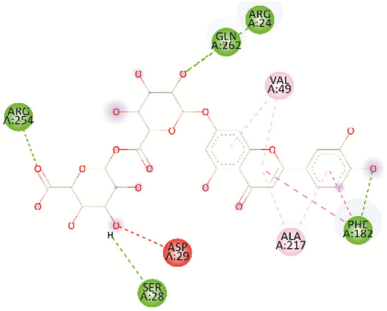
240	–9.2	PHE182, ALA217, TYR46, VAL49	ARG221, LYS120, SER216	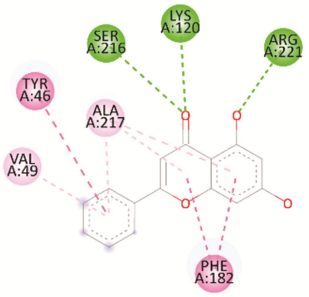
JTT	–7.4	PHE182, ALA217, TYR46, VAL49, MET258, ASP29		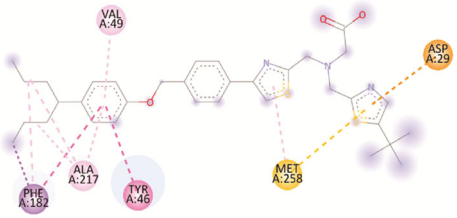

Considering the binding energy and vital amino acid interaction the 3 hits complexes PTP1B-136, PTP1B-216 and PTP1B-217 were identified and subjected to 100 ns MD simulation. MD was performed to predict the conformational stability of the ligand within the active site of the target. The dynamic nature of the complex was analysed by RMSD, RMSF, Rg, number of hydrogen bond, and number of interactions within the protein ligand complex. RMSD value indicate the average change in movement of a sample of atoms for a specific time frame with respect to the reference frame. It is computed for all the frames in the trajectory. RMSD value is a measure of the degree of stability of the target-ligand complex. Higher the RMSD value lesser is the target-ligand complex stability. The RMSD of the PTP1B-IN, PTP1B-136, PTP1B-216 and PTP1B-217 complexes was plotted against the MD simulation

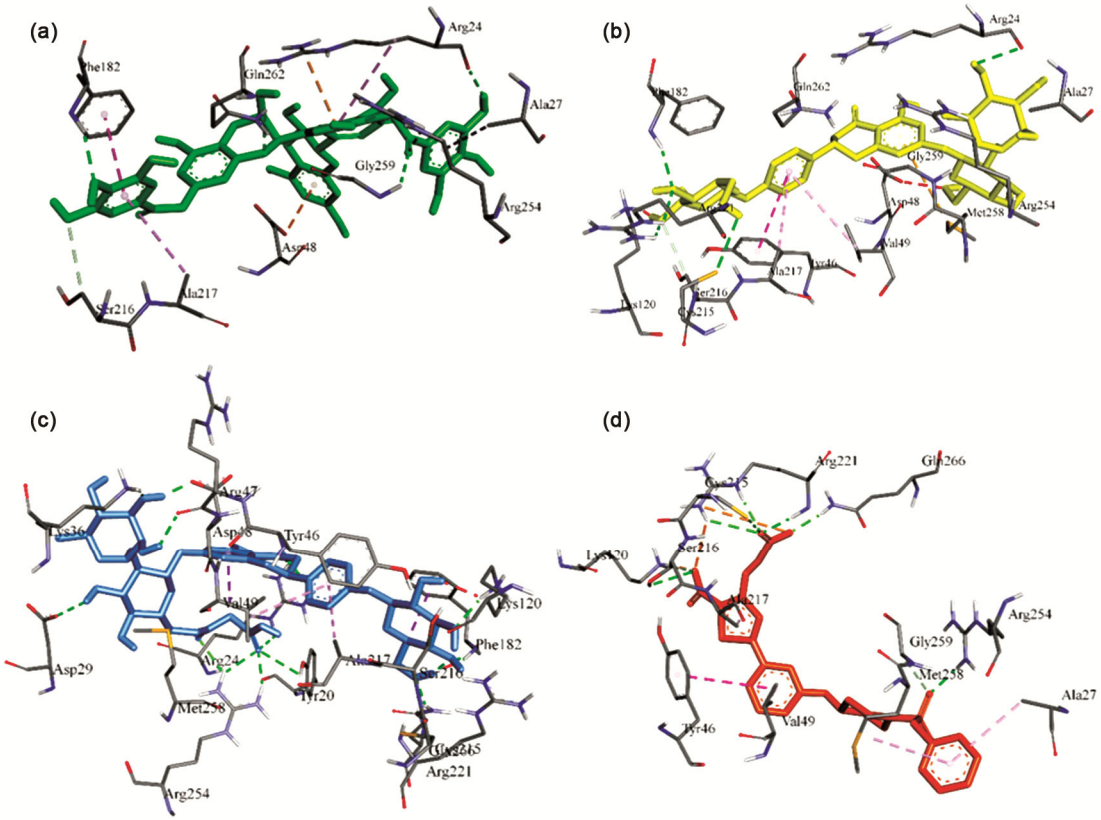

Fig. 3 — 3D interaction of PTP1B with reference inhibitor and selected polyphenols. A) interaction of IN with PTP1B. B) interaction of 136 with PTP1B. C) interaction of 216 with PTP1B. and D) interaction of 217 with PTP1B.

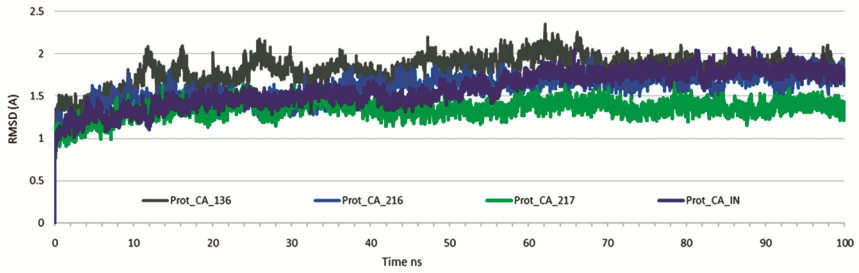

Fig. 4 — Molecular dynamic RMSD of PTP1B-IN, PTP1B-136, PTP1B-216 and PTP1B-217 complexes.

time, as shown in Fig. 4. The average RMSD in the PTP1B-IN, PTP1B-216 and PTP1B-217 complexes was found to be 1.60 Å,1.58 Åand1.34 Å, respectively. The RMSD of the complexes increased initially up to 20 ns and then remained stable up to 45 ns. Later slight increase in the RMSD was observed for remaining simulation. However, for PTP1B-136 complex, the RMSD fluctuated initially for first 30 ns and then became stable for the rest of the simulation duration. The average RMSD was about 1.81 Å. In comparison to the reference, two complexes PTP1B-216 and PTP1B-217 are the most stable.

RMSF is useful for depicting confined changes along the protein chain. Greater RMSF values implies a higher amount of mobility and instability of the ligand in the receptor, whereas lower RMSF values indicate stability and rigidity. The average RMSF for PTP1B-IN, PTP1B-136, PTP1B-216 and PTP1B-217 complexes are 0.848 Å, 0.8225 Å,0.7747 Å and 0.673 Å,respectively as shown in Fig. 5. In conclusion, as the observed average RMSF values of receptor amino acid residues are lower when it binds with the natural polyphenols compounds as compared to the reference inhibitor suggesting that PTP1B forms stable and

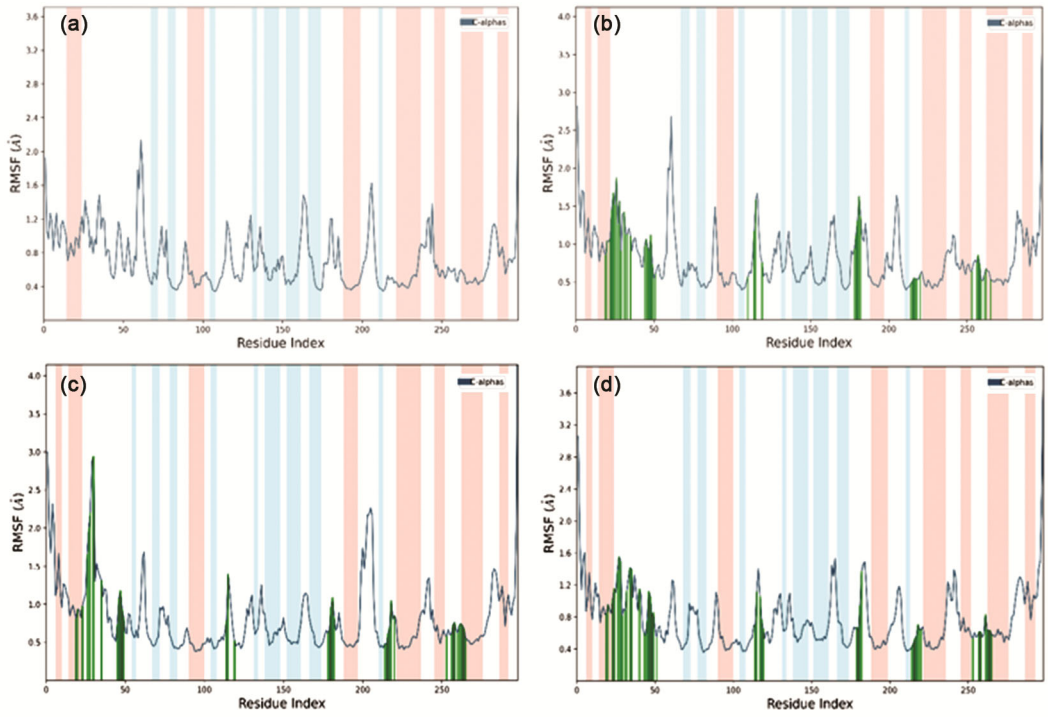

Fig. 5 — Molecular dynamic RMSF A) PTP1B-136. B) PTP1B-216. C) PTP1B-217 and D) PTP1B-IN complexes.

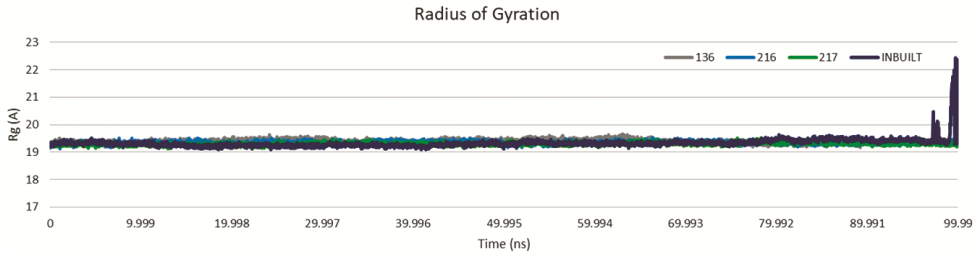

Fig. 6 — Radius of gyration (Rg) for PTP1B-IN, PTP1B-136, PTP1B-216 and PTP1B-217 complexes

rigid complexes with natural polyphenols compounds. Rg denotes the degree of protein compaction. A higher value suggests a less compact protein. Rg's trajectory analysis displays the overall change of the protein's dimension throughout dynamics. The average Rg value for PTP1B-IN, PTP1B-136, PTP1B-216 and PTP1B-217 complexes are 19.33 Å, 19.39 Å, 19.34 Å and 19.30 Å, respectively as shown in Fig. 6. The data indicate that the ligands have established compact and stable complexes with the PTP1B protein.

H-bond play a significant role in the development of stable connection between ligand and receptor. In complex PTP1B-136, H-bond interactions with ARG24, GLY259, ARG254, GLN262, and SER216 were retained, whereas new polar interaction with ASP29 & PHE30, new hydrophobic bond interaction with PHE182 were observed. Water bridges were formed at GLN262, LYS36, ASP48 and SER50 as shown in Fig. 7a. In complex PTP1B-216, H-bond interactions with ARG24 was retained and new polar interaction with ASP181, GLN262, GLN 266, LYS120, ASP48 and ASP29 was observed. Additionally, new hydrophobic bond interaction was observed with ILE219, whereas it was retained with VAL49, TYR46 and MET258. Water bridges were formed at ASP48, ASP29, ASP262 and ASP181as shown in Fig. 7b. In complex PTP1B-217, polar interactions with GLN266, ARG24, ASP48, LYS36, ASP29, TYR20 and LYS120 were retained. New hydrophobic bond interaction was observed with ILE219, VAL49 and MET258, whereas it was retained with TYR46, PHE182 and ALA217. Water bridges were formed at ASP48, ASP29, PHE30,

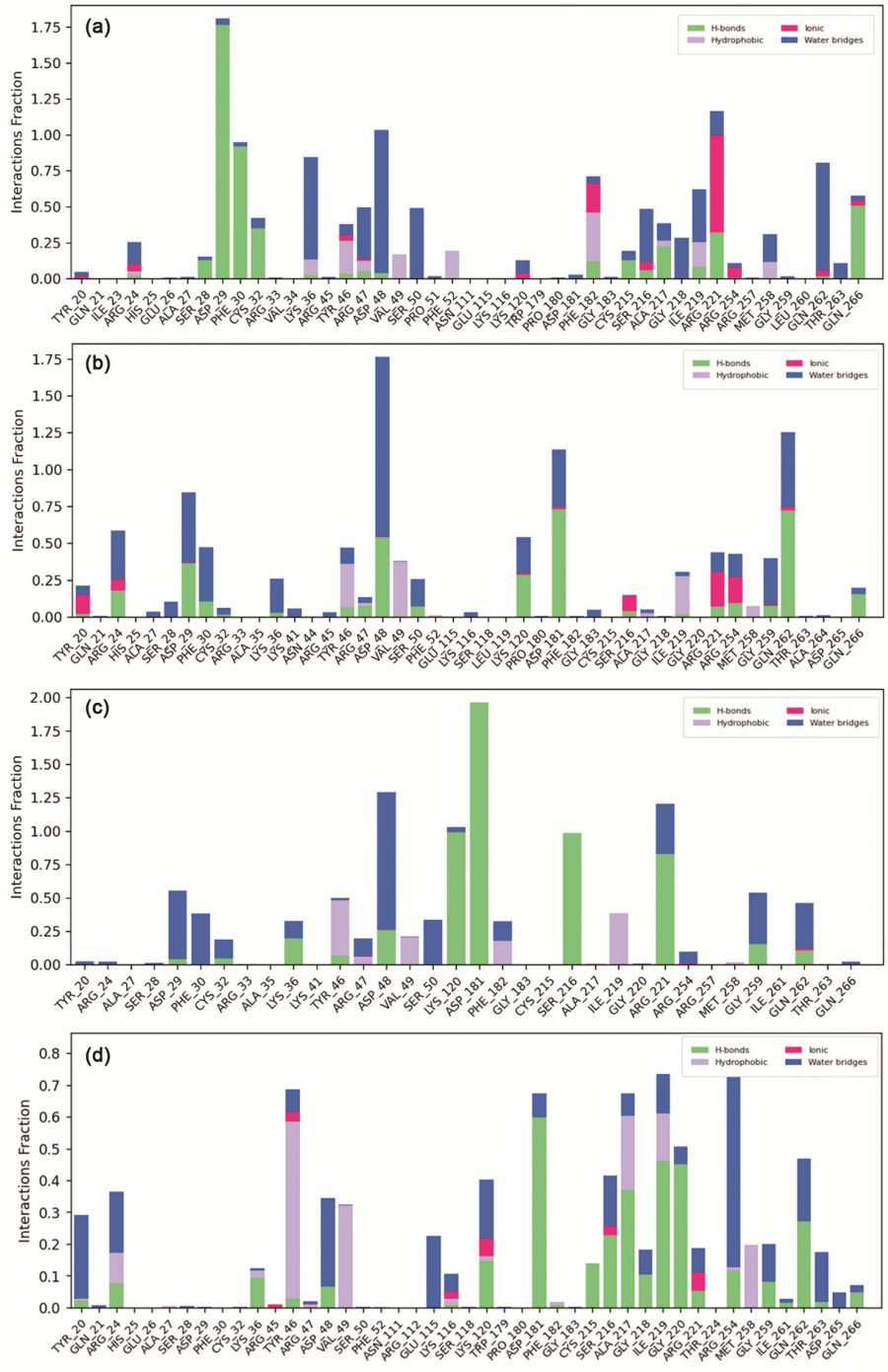

Fig. 7 — The plot represents protein-ligand contacts of complexes. A) PTP1B-136. B) PTP1B-216. C) PTP1B-217 and D) PTP1B-IN. with respect to residues of PTP1B during 100 ns MD simulation.

CYS32, GLN259 and GLN262 as shown in Fig. 7c. Above data suggest that ligands 136 and 217 have created a larger number of stable H-bonds as compared to the reference ligand as shown in Fig. 7c at active site of PTP1B (Fig. 7d) during the complete MD simulation.

Conclusions

Nowadays, *in silico* methodologies are playing crucial role in the drug discovery, as well as in identification and optimization of promising lead molecules. These methods are time saving and cost effective. In the present study, techniques like

molecular docking and dynamic simulation have been employed to discover natural polyphenols as potential PTP1B inhibitors. After analysing the molecular docking and dynamic simulation data, we predict three natural polyphnenols viz, PTP1B-136, PTP1B-216 and PTB1B-217 as possible PTP1B inhibitors for the management of T2D. However, *in-vitro* and *in-vivo* data are required to further validate the activity of the selected polyphenols.

Supplementary Information

Supplementary information is available in the website http://nopr.niscpr.res.in/handle/123456789/58776.

References

1 Balaji R, Duraisamy R, &Kumar M P, *Drug Invention Today*,12 (2019) 98-103.
2 Sun H, Saeedi P, Karuranga S, Pinkepank M, Ogurtsova K, Duncan B B, Stein C, Basit A, Chan J C N, Mbanya J C, Pavkov M E, Ramachandaran A, Wild S H, James S, Herman W H, Zhang P, Bommer C, Kuo S, Boyko E J & Magliano D J,*Diab Res Clin Pract,* 183 (2022) 109119.
3 Rachdaoui N, *Int J Mol Sci*, 21 (2020) 1770.
4 Gastaldelli A, *Diab Res Clin Pract*, 93 (2011) S60.
5 Hao J, Han L, Zhang Y & Wang T, *Evid-Bas Comp Alt Med*, 2020 (2022) 1057648. (https://doi.org/10.1155/2020/1057648).
6 Mocciaro G & Gastaldelli A, *Hand Exp Pharm*, 274 (2022) 145.
7 Asante-Appiah E & Kennedy B P, *Am J Phys End Met*, 284 (2003) E663.
8 Zhang Z Y, Dodd G T & Tiganis T, *Trends Pharm Sci*, 36 (2015) 661.
9 Tiganis T, *FEBS J*, 280 (2013) 445.
10 Elchebly M, Payette P, Michaliszyn E, Cromlish W, Collins S, Loy A L, Normandin D, Cheng A, Himms-Hagen J, Chan C C, Ramachandran C, Gresser M J, Tremblay M L & Kennedy B P, *Science*, 283 (1979) 1544.
11 Koren S & Fantus I G, *Best Pract Res Clin Endo Met*, 21 (2007) 621.
12 Chen P J, Cai S P, Huang C, Meng X M & Li J, *Toxicology*, 337 (2015) 10.
13 Liu R, Mathieu C , Berthelet J , Zhang W, Dupret J-M, Liu R, Mathieu C, Berthelet J, W Zhang, Dupret J-M & Rodrigues L F, *Int J Mol Sci*, 23 (2022) 7027.
14 Shehadeh M B, Suaifan G A R Y & Abu-Odeh A M, *Molecules*, 26 (2021) 4333.
15 Uddin Z, Song Y H, Ulla M, Z Li, Kim J Y & K H Park, *Front Chem*, 6 (2018) 335887.
16 Ha M T, Park D H, Shrestha S, Kim M, Kim J A, Woo M H, Choi J S & Min B S, *Fitoterapia*, 131 (2018) 119.
17 Noshita T, Kakizoe Y, S Tanabe, Ouchi H & Tai A, *Lett Org Chem*, 17 (2020) 939.
18 Lou Y, Su S Y, Li Y N, Lei C, Li J Y & Hou A J, *J Fitoterapia*, 44 (2019) 88.
19 McConkey B, Sobolev V & Edelman M, *Curr Sci*, 83 (2002) 845.
20 Pantsar T & Poso A, *Molecules*, 23 (2018) 1899.
21 Hollingsworth S A & Dror R O, *Neuron*, 99 (2018) 1129.
22 Durrant J D & McCammon J A, *BMC Biol*, 9 (2011) 1.
23 Rothwell J A, Perez-Jimenez J, Neveu V, Medina-Remón A, M'Hiri N, García-Lobato P, Manach C, Knox C, Eisner R, Wishart D S & Scalbert A, *J Bio Database Cur*, 2013 (2013) bat070. (https://doi.org/10.1093/database/bat070).
24 Burley S K, Bhikadiya C, Bi C, Bittrich S, Chao H, Chen L, Craig P A, Crichlow G V, Dalenberg K, Duarte J M, Dutta S, Fayazi M, Feng Z, Flatt J W, Ganesan S, Ghosh S, Goodsell D S, Green R K, Guranovic V, Henry J, Hudson B P, Khokhriakov I, Lawson C L, Liang Y, Lowe R, Peisach E, Persikova I, Piehl D W, Rose Y, Sali A, Segura J, Sekharan M, Shao C, Vallat B, Voigt M, Webb B, Westbrook J D, Whetstone S, Young J Y, Zalevsky A & Zardecki C, *Nucle Acids Res*, 51 (2023) D488.
25 Zhang Y & Du Y, *Future Medicinal Chemistry*, 10(2018) 2345-67.
26 Rao S N, Head M S, Kulkarni A & LaLonde J M, *J Chem Inf Model*, 47 (2007) 2159.
27 Talluri S, *Comb Chem High Thro Scr*, 24 (2020) 716.
28 Trott O & Olson A J, *J Comp Chem*, 31 (2010) 455.
29 Yahaya M A F, Bakar A R A, Stanslas J, Nordin N, Zainol M&Mehat M Z, *BMC Biotech*, 21 (2021) 38.
30 Patel CN, Jani SP, Jaiswal DG, Kumar SP, Mangukia N, Parmar RM, Rawal R M & Pandya H A,*Scientific Reports*, 11 (2021)20295.
31 Majumder R & Mandal M, *J Biomol Struct Dyn*, 40 (2022) 696.
32 Selvaraj C, Priya R B, Lee J K & Singh S K, *RSC Adv*, 5 (2015) 100498.
33 Gopinath P & Kathiravan M K, *RSC Adv*, 11 (2021) 38079.
34 Li D D, Wu T T, Yu P, Wang Z Z, Xiao W, Jiang Y & Zhao L G, *ACS Omega*, 5 (2020) 16307.
35 Singh S, Bansal A, Singh V, Chopra T & Poddar J, *J Diab Met Dis*, 21 (2022) 941.
36 Ala P J, Gonneville L, Hillman M, Becker-Pasha M, Yue E W, Douty B, Wayland B, Polam P, M L Crawley, McLaughlin E, Sparks R B, Glass B, Takvorian A, Combs A P, Burn T C, Hollis G F & Wynn R, *J Bio Chem*, 281 (2006) 38013.
37 Goldstein B J, Bittner-Kowalczyk A, White M F & Harbeck M, *J Bio Chem*, 275 (2000) 4283.
38 Andersen J N, Mortensen O H, Peters G H, Drake P G, Iversen L F, Olsen O H, Jansen P G, Andersen H S, Tonks N K& Møller N P H, *Mol Cell Biol*, 21 (2001) 7117.
39 Jung H A, Cho Y S, Oh S H, Lee S, Min B S, Moon K H & Choi J S, *Arch Pharm Res*, 36 (2013) 957.
40 Zhang X, Jiang H, Li W, Wang J & Cheng M, *Comp Math Methods Med*, 2017 (2017) 4245613. (https://doi.org/10.1155/2017/4245613).